

Cumulative Damage Assessment to Airdrop Vehicle Hull for the Landing Process

HE JIAN, MA JI-SHENG, WU DA-LIN, DENG SHI-JIE

Theory and Technology Department of Mechanic

Mechanical Engineering Colleague

Shijiazhuang He-ping West Road No.97

China

hejian108@163.com

Abstract:- In order to test the shock and vibration resistance performance of an airdrop vehicle, one test way is by actual equipment airdrop, but this way needs large human and financial resources and the experimental conditions can not be controlled well, numerical simulation analysis become another effective way. This article first built the dynamic model of the whole vehicle based on virtual prototype technology, analysis the airbag force at vehicle landing process by tools of finite element method, next did the dynamic simulation to the vehicle landing process and got the loads time history on the hull, then applied these loads on the finite element model of the hull and did the transient dynamic response to the model, got the stress and strain time history of the hull, last did the cumulative damage assessment based on the strain time history of the hull combined the Lemaitre damage model and the material parameter. The calculation results show that the damage variable D has a linear relationship with the number of landing times and after 6 times of limit landing process, the part of hull will failure. The research can provide reference to the shock and vibration test for large airdrop equipment.

Key-words: -Airdrop vehicle; Dynamic; Finite element; Shock; Damage Assessment

1. Introduction

Local war under the informatization condition has the characteristics of suddenly, high strength and high technology, airdrop operations is becoming more and more important for its quick response and strike capability.[1-2] To examine the shock and vibration resistance performance of the airdrop equipment, it must conduct the shock and vibration test to the equipment and do damage assessment to verify that if the equipment can work properly after landing process[3]. One way is by actual equipment airdrop, but this way has some weakness, one is the actual equipment airdrop experiment needs long time to prepare and costs much money, another is the experiment condition can not be controlled and it can't

systemically and comprehensive assessment the equipment performance under different landing conditions. [4-5] The use of simulation is not be affected by time and test environment and can analysis various conditions, so it is becoming an effective way[6].

The hull of airdrop vehicle impact with the ground directly at landing process and suffer large load from ground, so the article take the hull of airdrop vehicle as the research object. First built the virtual prototype model of whole airdrop vehicle based on the automatic dynamics analysis mechanical software ADAMS, got all loads on the hull through dynamic simulation. Then built the finite element

model of the hull in software PATRAN, applied all loads on the hull model and did the transient dynamic response to the model by NASTRAN software. Last, did the cumulative damage assessment based on the strain time history of the hull combined the Lemaitre damage model and the material parameter. The whole analysis process as shown in figure 1.

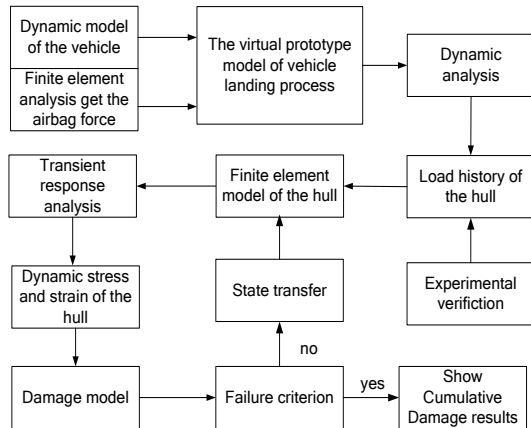


Fig .1 The analysis process

2. The virtual prototype model

The vehicle are mainly aked up by three parts, fire system, track system and auxiliary system[7]. This paper built the hull and track system by ADAMS software and it mainly contain the drive part and suspension system not include power and transmission parts. The track system have two sides and there are one sprocket, five road wheels, three support rolls, one idler and ninety-six belts of each side. The final Virtual prototype model of vehicle has a total of 257 bodies and 1194 degrees of freedom.

2.1 The main mechanical force model of vehicle

2.1.1 Nonlinear contact force model

The contact force of the vehicle mainly include the contact between belt and ground, sprocket, road wheel, idler and support roll, and the contact of two bodies for their clearance.

Based on Hertz elastic contact theory, the contact force between two objects is a nonlinear function of penetration depth and can be expressed like $F_n = K\delta^n$ [8] , but the Hertz contact force model do not account the energy dissipation process that

characterizes the contact-impact events in mechanical systems[9] . So the paper use the contact force model by the elastic Hertz’s law combined with a nonlinear viscoelastic element expressed as[10]

$$\begin{cases} F_n = K \cdot g^n + c \frac{dg}{dt} \\ c = step(g, 0, 0, d_{max}, c_{max}) \end{cases} \quad (1)$$

where K and n are the contact stiffness parameter and the nonlinear power exponent determined from material and geometric properties of the local region of the contacting objects, g is the penetration depth, c_{max} is the maximum damping coefficient, d_{max} denotes the penetration depth at which the damping get full. $step(\cdot)$ is the function approximates the Heaviside step function with a cubic polynomial.

For the numerical value of the above parameter, if the contact between two spherical body then the contact stiffness can be expressed like[11]

$$K = \frac{4}{3} E^* \sqrt{\frac{R_i R_j}{R_i + R_j}} \frac{1}{E^*} = \frac{1 - \mu_i^2}{E_i} + \frac{1 - \mu_j^2}{E_j} \quad (2)$$

in which E_i and μ_i are the Young’s modulus and Poisson’ ratio associated with each sphere. If the contact between a sphere i and a plane surface body j , the contact stiffness parameter depends on the radius of the sphere and the material prop ties of the contacting surfaces, being expressed as[9]

$$K = \frac{4}{3} E^* \sqrt{R_i} \quad (3)$$

The general number of n is 1.5, c_{max} is one percent of K and d_{max} is always 0.01 millimeter.

2.1.2 Nonlinear oil gas suspension dynamic model

Oil gas suspension are made up by a power cylinder and a accumulator, it transfers the pressure through the oil liquid and takes gas as the elastic element[7] . When the road wheel swing on the uneven road, it transfers the pressure to the accumulator by the oil liquid and releases the vibration energy by compressing the gas. The

characteristic of oil gas suspension is nonlinear and it changes with the compressed gas's trip.

According to the characteristics of the oil gas suspension, there uses a two-way torque to simulate the suspension[12] . The nonlinear of the two-way torque mainly for the gas polytropic index. Supposing that the displacement of the piston of power cylinder is s , then the force can be expressed as

$$F = -p_0 \left(\frac{A_2 s_0}{A_2 s_0 - A_1 s} \right)^m - c \dot{s} \quad (4)$$

Where p_0 is the initial pressure of accumulator, A_1 and A_2 are effective action area of power cylinder and accumulator, s_0 is the initial gas length of the accumulator, m is the gas polytropic index, c is the damper.

2.1.3 Nonlinear airbag force model

The airbag buffer process involves the issue of fluid-structure interaction between the gas and airbag boundary, calculation about the effect of airbag now mainly depends on the finite element method[13-16] and it can't simulate the airbag buffer process directly in software ADAMS. So the paper first did the simulation to airbag buffer process based on Control Volume(CV) method by software LS-DYNA and got the parameter of airbag such as airbag pressure, height and so on, then calculated the airbag force versus the airbag remaining height, and last built the nonlinear force model in software ADAMS to simulate the effect of airbag buffer process.

The buffer system of the vehicle contains eight airbags, there are air inlet at the bottom and exhaust port at the side on each airbag. In the process of vehicle falling, the air inflating into airbag by the bottom air inlet, at the landing process, the airbag remains close in the beginning and generates compressed to absorb energy, when pressure in the airbag increases to a predetermined threshold, the vent port opens, the gas inside the airbag vent to air for the energy dissipates.

The CV method has two basic assumptions one is that gas in the airbag meets the ideal gas equation and can use the classical thermodynamics equation, another is the temperature and pressure inside the airbag are equal everywhere. [17-20]

In software LS-DYNA, the element type of airbag is SHELL163 and the material is number 34 orthogonal anisotropic material MAT_FABRIC. The keyword defines airbag is AIRBAG_WANG_NEFSK , and the link between vehicle and airbag is through the keyword of CONSTRAINED_EXTRA_NODES_SET, the contact between airbag and ground is CONTACT_AUTOMATIC_SURFACE_TO_SURFACE.[21-23]

The whole finite element model of the airbag buffer system as shown in figure2 and the characteristics of airbag at landing process as shown in figure 3.

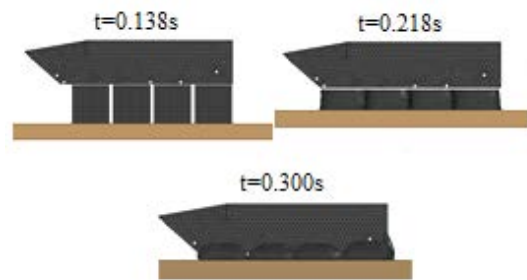


Fig.2 The finite element model of airdrop landing buffer system

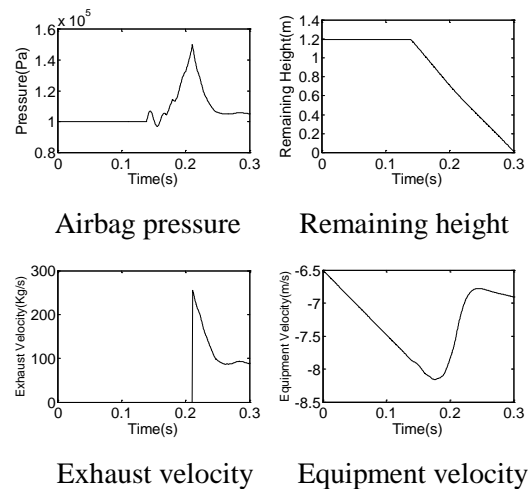


Fig.3 The airbag characteristics curve

From the figure 3 we can see that, at the beginning, the airbag free falls with the vehicle and the velocity of vehicle increases gradually, when the time airbag touches ground then the airbag is compressed and the airbag pressure increases, produces the upward force to the vehicle and the vehicle velocity reduces gradually, when the airbag pressure rises to the exhaust pressure then the exhaust port of airbag is open and the airbag begin

to exhaust gas to air, the airbag pressure reduces gradually, when the airbag pressure reduces to a certain point, the airbag force small than the vehicle gravity and the vehicle velocity further increases. Calculated the airbag force versus the airbag remaining height curve as shown in figure 4. In the software ADAMS, completed the airbag force model by the AKISPL function.

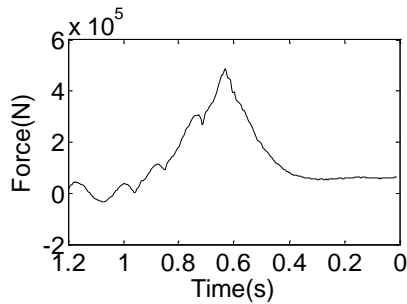


Fig.4 The airbag cushion force versus the airbag remaining height

Last, the final virtual prototype model of the airdrop vehicle landing process in the ADAMS as shown in figure 5.

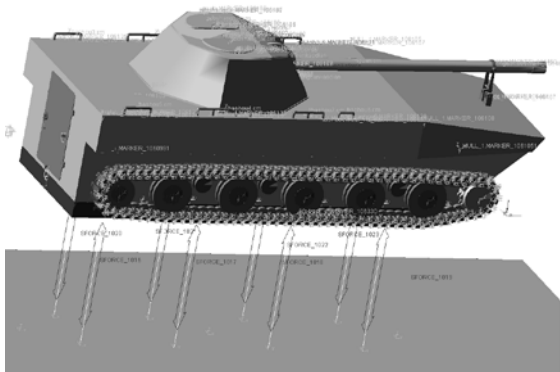


Fig.5 The virtual prototype model of airdrop vehicle landing process

3.The load time history

3.1 The load time history of hull at landing process

Through dynamic simulation analysis to the whole virtual prototype model of the airdrop vehicle landing process, got the 23 force load on the vehicle hull, these force contain the contact force between hull and ground, turret and track system wheels. The typical load time history on the hull at the landing process as shown in figure 6 and figure 7, the figure 6 shows the

contact force between hull and ground, turret, the figure 7 shows the torque at the joint of the first order road wheel of left track system with hull.

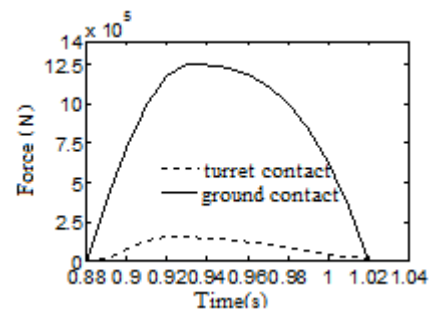


Fig.6 The contact force

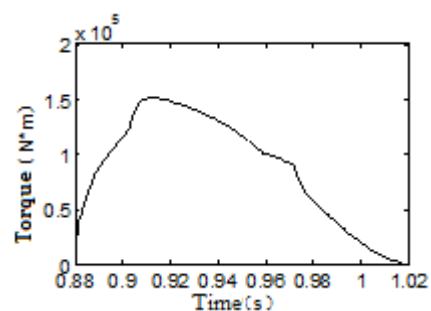


Fig.7 The torque

3.2 The experimental verification to the dynamic model of vehicle

To verify the effectiveness of the virtual prototype model of airdrop vehicle landing process, took the typical landing condition of real equipment airdrop experiment as the test condition. According to the general landing velocity of hull, put the vehicle into height of 3.8 meter and dropped it down, Through dynamics simulation to airdrop vehicle landing process, got the shock acceleration curves of two typical parts, hull and turret, compared the simulation results with the measured signal of real equipment airdrop experiment, the acceleration sensor layout in the bottom center of hull and the back deck of turret. The comparison of the simulation and experiment acceleration results as shown in table 1.

From the comparison of simulation and experiment, we can see that the peak acceleration and contact time of the test location got from simulation has high similarity with the experimental test, and the max error is not more than nine percent, it shows that the dynamic model of vehicle has a well

response characteristic and can be used for engineering simulation analysis.

Tab.1 The acceleration comparison of simulation and experiment

	Test location	Simulation	Experiment	Error
Peak acceleration	Bottom hull	14.7g	14.3g	2.8%
	Back turret	16.8g	16.3g	3.1%
Contact time	Bottom hull	0.140s	0.152s	8.6%
	Back turret	0.150s	0.158s	5.3%

4. Transient response analysis

4.1 The finite element model of hull

Imported the three-dimensional hull model to the software PATRAN, and used quadrilateral shell element to mesh the hull body, used tetrahedron solid element to mesh the column. The whole model has total 33390 nodes and 99456 elements.

The Elastic modulus of the material is 7.02E10Pa, the Poisson' ratio is 0.3, the Yield limit is 4E8Pa and the Damping coefficient of material is 0.005. Built the time dependent load case, and defined the loads and displacement constraint under the time dependent load case. Put the dynamic load time history in form of nonlinear field by nonlinear spatial fields in the PATRAN. For the torque in the figure 6, transfer the torque into force according to the length of balance elbow. Last the final finite element model as shown in figure 8. The figure 8 shows the loads condition of 0.005 seconds after vehicle touch the ground.

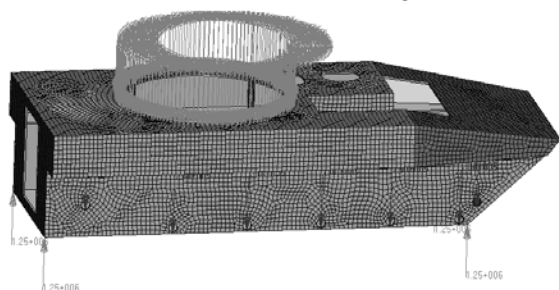


Fig.8 Finite element model of hull

4.2 The transient response analysis settings

The generalize coordinate expression of transient response analysis can be expressed as[24-25]

$$M \ddot{x} + C \dot{x} + Kx = P \quad (5)$$

where M represents the mass matrix of system, C is the damping matrix, K is the stiffness matrix, P is the external load matrix and x is the displacement vector. The mass matrix, stiffness matrix and external matrix of system are easily be confirmed, the difficulty is calculating the damping matrix of system, the damping matrix can be expressed as

$$C = C_1 + C_2 + \frac{G}{\omega_3} K + \frac{1}{\omega_4} \sum G_E K_E \quad (6)$$

where C_1 and C_2 are external damping matrix of system, G is the structure damping coefficient, ω_3 is the transformation coefficient which transfer the structure damping to viscous damping, G_E is element structure damping coefficient, K_E is the element stiffness matrix and ω_4 is the transformation coefficient which transfer the element structure damping to viscous damping.

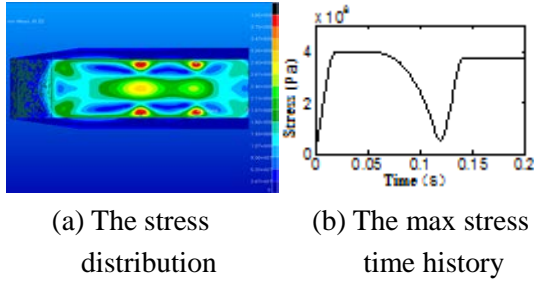
For the horizontal velocity of the vehicle is small at the landing process and the friction is small, so let the C_1 and C_2 be 0 and mainly considered the structure damping. Through modal analysis to the hull, got the first order modal frequency is 78.369Hz, so $\omega_3 = \omega_4 = 2\pi f = 492.4 \text{ rad/s}$. Took the structure damping as 0.005.

4.3 The stress and strain results of hull

Did the transient response analysis to the finite element model of hull by NASTRAN solver, the simulation results shows that the max Von Mises stress mainly concentrates on the bottom of column and bottom surface of hull at the vehicle landing process. The max stress reaches the yield limit 400Mpa and gradually decreases as the load decreases, at end it keeps about 375 Mpa remanent stress. The stress response results as shown in figure 9.

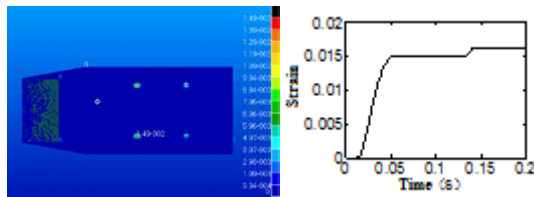
Did the plastic strain analysis to the hull based on the stress results, the figure 10 shows the plastic strain results of hull. The calculated results shows

the hull occur some plastic strain at the normal landing process and the plastic strain of major area of hull is small, the large plastic strain concentrate on the column around and the max plastic strain appears at the bottom of right front column and it achieve 1.61%.



(a) The stress distribution (b) The max stress time history

Fig.9 The stress results



(a) The plastic strain distribution (b) The max plastic strain time history

Fig.10 The plastic strain results

5. Cumulative Damage Assessment

5.1 Lemaitre damage model[26-27]

In 1997, Jean Lemaitre proposed a model of damage evolution based on a thermodynamic framework, for this model, in the case of isotropic damage, the scalar variable D represents the ratio of micro-void area δS_D to total area δS , $D = \delta S_D / \delta S$. $D = 0$ corresponding to the undamaged state and D equal D_c corresponding to local failure.

The evolution law of damage D is:

$$\dot{D} = (Y / S_0)^{s_0} \dot{p} \quad (7)$$

$$Y = \frac{\sigma_{eq}^2}{2E(1-D)^2} \left\{ \frac{2}{3}(1+\nu) + 3(1-2\nu) \left(\frac{\sigma_H}{\sigma_{eq}} \right)^2 \right\} \quad (8)$$

where S_0 and s_0 are also damage parameters, σ_{eq} is the Von Mises equivalent stress, σ_H / σ_{eq} is the triaxiality index. p is the Cumulative plastic strain.

According to the Ramberg-Osgood hardening rate:

$$\sigma_e / (1 - D) = K p^{1/M} \quad (9)$$

where K and M are also material hardening exponents.

Put the equation (8) and (9) into (7) and we can get that

$$\dot{D} = \left\{ \frac{K^2}{2ES_0} \left[\frac{2}{3}(1+\nu) + 3(1-2\nu) \left(\frac{\sigma_H}{\sigma_{eq}} \right)^2 \right] \right\}^{s_0} p^{\frac{2s_0}{M}} \dot{p} \quad (10)$$

To metallic material, the M is large however s_0 has a order of magnitudes with 1, so integral to equation(10) and we can get

$$D = \left\{ \frac{K^2}{2ES_0} \left[\frac{2}{3}(1+\nu) + 3(1-2\nu) \left(\frac{\sigma_H}{\sigma_{eq}} \right)^2 \right] \right\}^{s_0} (p - p_0) \quad (11)$$

in which, p_0 corresponding to the plastic strain threshold, when $p \leq p_0$, the scalar variable D is 0, when $p = p_c$, the damage achieve to limit and $D = D_c$, so there is

$$D = D_c \frac{(p - p_0)}{(p_c - p_0)} \quad (12)$$

In the uniaxial case of isotropic damage, for the large plastic strain, there is $p \approx \varepsilon$, so equation (12) can be written as

$$D = D_c \frac{(\varepsilon - \varepsilon_0)}{(\varepsilon_c - \varepsilon_0)} \quad (13)$$

where the ε_0 and ε_c are strain corresponding to the damage threshold and limit. From equation (13) we can see that the damage D linear changes with strain and can be shown as figure 11.

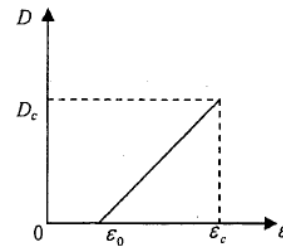


Fig.11 The evolution curve of damage under case of uniaxial stress

To be identified the Lemaitre model needs four

independent parameters, D_0 , D_c , ε_0 , ε_c and it is possible to obtain all of them from a single tensile test conducted using the procedure described in [28-29], Essentially, it is based on Young's modulus estimation for each unloading cycle performed during a tensile test. This procedure allows evaluation of the reduction of Young's elastic modulus while plasticization takes place. In fact, it can easily be shown that

$$D = 1 - \frac{\tilde{E}}{E} \tag{14}$$

where \tilde{E} is the elastic modulus of the damaged material that has to be measured during all the tensile tests. From the paper [30], we can get the damage parameters of the hull material as shown in table 2.

Tab.2 Lemaitre's model parameters for hull material

D_0	D_c	ε_0	ε_c
0	0.304	0	0.0834

5.2 Cumulative damage assessment of hull after many times landing process

5.2.1 Cumulative damage assessment of hull for normal landing condition

To analysis the cumulative damage rule of the hull after many times landing process, used the method of figure 1, did 10 times simulation to the hull for normal landing condition.

Tab.3 The damage variable D under normal landing condition

Times	Max plastic strain	Change of plastic strain	Damage D
1	1.61%		0.059
2	1.86%	0.25%	0.068
3	2.10%	0.24%	0.077
4	2.34%	0.24%	0.085
5	2.58%	0.24%	0.094
6	2.82%	0.24%	0.103
7	3.06%	0.24%	0.110
8	3.30%	0.24%	0.120
9	3.55%	0.25%	0.129
10	3.79%	0.24%	0.138

Calculated the max plastic strain of the hull after landing process, combined the equation (13) and calculated the damage variable D, the simulation results as shown in table 3. The evolution of damage D for normal landing condition as shown in figure 12 of the curve a.

From the calculation results, we can see that the plastic strain is not unchanged under the same impact load, but there is a trend of gradual growth. As the figure 11 shows, under the same impact load, the cumulative damage variable D has a linear relationship with the number of landing times.

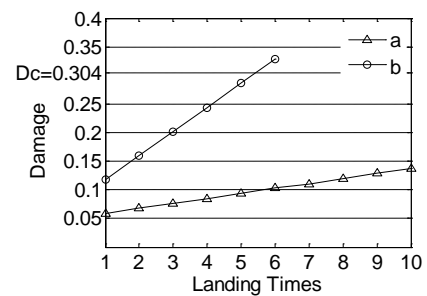


Fig.12 The evolution of damage D versus the landing times

5.2.2 Cumulative damage assessment of hull for limit landing condition

In order to further research the damage of hull under the limit landing condition, according to the airdrop equipment index, the max impact acceleration can not exceed 20g, so here assuming the max impact acceleration is 20g of limit landing condition, the acceleration curve as shown in figure 13.

Tab.4 The damage variable D under limit landing condition

Times	Max plastic strain	Change of plastic strain	Damage D
1	3.23%		0.118
2	4.39%	1.16%	0.160
3	5.54%	1.15%	0.202
4	6.70%	1.16%	0.244
5	7.85%	1.15%	0.286
6	8.99%	1.14%	0.328

The cumulative damage assessment of hull for limit landing condition simulation results as shown in table 4. The evolution of damage D for limit

landing condition as shown in figure 12 of the curve b. From the calculation results we can see that after 6 times landing process for limit landing condition, the part of hull will failure.

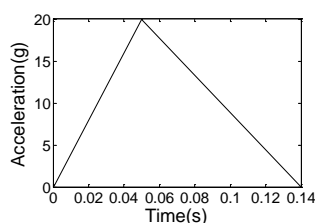


Fig.13 The acceleration curve

5.2.3 The damage comparison of normal and limit landing condition

To find out the influence of the peak acceleration value to the hull damage, now compare the damage value under normal and limit landing condition as shown in table 5.

Tab.5 The comparison of damage under normal and limit landing condition

	Peak acceleration	First time damage	Change of damage after first time
Normal	14.7g	0.059	0.24%
Limit	20g	0.118	1.15%
Change	36%	100%	379%

6. Conclusion

1. This paper through dynamic simulation to get the loads, transient response analysis to the finite element model and combine the Lemaitre damage model, do the cumulative damage assessment to the vehicle hull, the whole analysis process can provide reference to the large airdrop equipment test.
2. Through the transient response analysis to the finite element model of hull, we find out that the weakness part of the hull is the column bottom, this can provide the basis to the structure strengthen or weight reduction design of the hull.
3. Through analysis to Lemaitre damage model, get the damage variable D linear changes with the strain of material.
4. From the research, we find out under the same

impact load, the cumulative damage variable D has a linear relationship with the number of landing times.

5. From the table 5, we can see that when the peak acceleration which hull suffers changes 36 percent, the first time landing damage changes 100 percent and the change of damage after first landing process reaches 379 percent, so the damage of the hull is nonlinear with the acceleration which suffers but has a almost index increase relationship with the acceleration. So it is necessary to reduce the shock acceleration which vehicle suffers by buffer device at the landing process.

6. The cumulative damage calculation results shows after 6 times limit landing process, the part of hull will failure, so the airdrop life of vehicle is not less than 6 times.

References

- [1] LI Chang-ying, WANG Xuan-min, YANG Jin, The present status and development trend of foreign airborne combat vehicle, Journal of Guilin Air Force Academy, 2010, 27(1):22-25.
- [2] HAO Guang-qing, Present situation and development of heavy equipment airdrop technology at home and abroad, The tenth national safety lifesaving society exchange Conference set, 2006, 109-112.
- [3] HE Qing, The overall scheme design of airborne multiple rocker launcher, Nanjing University of Science and Technology, 2006
- [4] SUN Hong-hai, DIAO Zeng-xiang, WANG Xi-an-ning, On the research and development of military vehicles airdrop, Academy of Military Transportation, 2004, 6(1).
- [5] TAN Jun, HAN Xu, LIU Xin, Numerical analysis and improvement of airdrop landing process of special vehicles, Packaging Engineering, 2010, 01:57-61.
- [6] LIU Xia, QI Huan, CHEN Ying-chun, Simulation of the impact response of airdropping cargo, Packaging Engineering, 2005, 26(5):57-61.
- [7] ZHANG Pei-lin, HE Zhong-bo, LV Jian-gang,

The structure and principle of the vehicle ,
National Defence Industry Press, 2007.

- [8] K.L.Johnson, One hundred years of Hertz contact, Proceedings of the Institution of Mechanical Engineers 196(1982): 363–378.
- [9] Margarida Machado, Pedro Moreira, Paulo Flores, Compliant contact force models in multi-body dynamics:Evolution of the Hertz contact theory, Mechanism and Machine Theory53 (2012)99-121
- [10] MSC. Software-MSC.ADAMSUsers'Guide.
- [11] Andre' Roy, Juan A.Carretero, A damping term based on material properties for the volume based contact dynamics model, International Journal of Non-Linear Mechanics, 47(2012) 103-112.
- [12] WU Da-lin, MA Ji-sheng, DONG Zi-wei, Vibration analysis of suspension system of self-propelled gun based on ADAMS, Journal of Vibration and Shock, 2005, 24(5):39-41.
- [13] LI Liang-chun, HUANG Gang, LI Wen-sheng, et al.Simulation analysis of new type landing cushion airbag based on ANSYS/LS-DYNA, Packaging Engineering, 2012, 33(5):16-20.
- [14] QI Ming-si, LIU Shou-jun, ZHAO Qi, et al.Simulation research on Landing Process of cushioning Airbag, Packaging Engineering, 2013, 34(23): 5-8.
- [15] WEN Jin-peng, LI Bin, YANG Zhi-chun, Progress of study on impact attenuation capability of airbag cushion system, Journal of Astronautics, 2010, 31(11):2438-2447.
- [16] YANG Wei, QI Ming-si, ZHANG Jiao, Research on punched quick airdrop cushion, Packaging Engineering, 2010, 31(5):106-108.
- [17] ZHANG Jun-yuan, LI Dong-jun, BI Ying, et al. Optimization of vehicle side curtain airbag module based on computer aided engineering, Chinese Journal of Mechanical Engineering, 2009, 22(4):521-527.
- [18] CHENG Han, Numerical Simulation Research on airbag Working Process, Nanjing University of Aeronautics and Astronautics, 2009
- [19] DAI Xiao-fang, Numerical simulation of airbag deployment based on fluid-structure interaction methodology, Dalian University of Technology 2007.
- [20] XU Jing-jing, Numerical simulation of airbag dynamic mechanical performance based on fluid-structure interaction approach, Dong Hua University, 2010.
- [21] GE Si-cheng, SHI Yun-tao.Study on cushioning characteristics of air bag for RPV recovery, Journal of Nanjing University of Aeronautics and Astronautic, 1999, 31(4): 458-463.
- [22] LE Yong-xiang, Numerical simulation and optimal design of the process of airbag landing, Hunan University, 2010.
- [23] CHEN Shuai, LI Bin, WENG Jin-peng, Cushioning characteristic and parameter design of a soft landing airbag, Journal of vibration and shock, 2009, 28(4):25-29.
- [24] YANG Xu-dong, ZHANG Shi-lian, Structure damper analysis in structure transient response with finite element method, China Offshore Platform, 2004, 19(2):30-34.
- [25] YU Bai-sheng, HUANG Wen-hu, ZHENG Gan-gtie, Damping calculating using universal finite element analytical software NASTRAN, Structure and Environment Engineering, 2003, 30(1):7-10.
- [26] A.Baldi, L.Francesconi, A.Medda, Comparing two damage models under shear stress, Experimental Mechanics, 2013, 53:1105-1116.
- [27] HUANG Jin, Research on forming limits of sheet metal basing on continuum damage mechanics, Wuhan University of Technology, 2006.
- [28] Lemaitre J, A continuous damage mechanics model for ductile fracture, J Eng Mater Technol, 1985, 107(2):83–89.
- [29] Lemaitre J, A course on damage mechanics, 2nd edn, Springer, Berlin.
- [30] LI Jian-yang, WANG Hong-yan, RUI Qiang, Research on cumulative damage assessment method for airborne vehicle at landing based on finite element analysis, Journal of System Simulation, 2014, 26(1):208-214.